

# Michaelis-Menten Quantification of Ligand Signaling Bias Applied to the Promiscuous Vasopressin V2 Receptor

✉ Franziska Marie Heydenreich, Bianca Plouffe, Aurélien Rizk, Dalibor Milić, Joris Zhou, Billy Breton, Christian Le Gouill, Asuka Inoue, ✉ Michel Bouvier, and Dmitry B. Veprintsev

Laboratory of Biomolecular Research, Villigen, Switzerland (F.M.H., A.R., D.M., D.B.V.); Department of Biology, Paul Scherrer Institute, Zürich, Switzerland (F.M.H., A.R., D.M., D.B.V.); Department of Biochemistry and Molecular Medicine, Institute for Research in Immunology and Cancer, Université de Montréal, Montréal, Québec, Canada (F.M.H., B.P., J.Z., B.B., C.L., M.B.); MRC Laboratory of Molecular Biology, Cambridge, United Kingdom (F.M.H.); The Wellcome-Wolfson Institute for Experimental Medicine, School of Medicine, Dentistry and Biomedical Sciences, Queen's University Belfast, Belfast, United Kingdom (B.P.); Department of Structural and Computational Biology, Max Perutz Laboratories, University of Vienna, Vienna, Austria (D.M.); Graduate School of Pharmaceutical Sciences, Tohoku University, Sendai, Japan (A.I.); Centre of Membrane Proteins and Receptors (COMPARE), University of Birmingham and University of Nottingham, Midlands, United Kingdom (D.B.V.); and Division of Physiology, Pharmacology and Neuroscience, School of Life Sciences, University of Nottingham, Nottingham, United Kingdom (D.B.V.)

Received February 10, 2022; accepted June 6, 2022

## ABSTRACT

Activation of G protein-coupled receptors by agonists may result in the activation of one or more G proteins and recruitment of arrestins. The extent of the activation of each of these pathways depends on the intrinsic efficacy of the ligand. Quantification of intrinsic efficacy relative to a reference compound is essential for the development of novel compounds. In the operational model, changes in efficacy can be compensated by changes in the “functional” affinity, resulting in poorly defined values. To separate the effects of ligand affinity from the intrinsic activity of the receptor, we developed a Michaelis-Menten based quantification of G protein activation bias that uses experimentally measured ligand affinities and provides a single measure of ligand efficacy. We used it to evaluate the signaling of a promiscuous model receptor, the Vasopressin V2 receptor (V2R). Using BRET-based biosensors, we show that the V2R engages many different G proteins across all G protein subfamilies in response to its primary endogenous agonist, arginine

vasopressin, including Gs and members of the Gi/o and G12/13 families. These signaling pathways are also activated by the synthetic peptide desmopressin, oxytocin, and the nonmammalian hormone vasotocin. We compared bias quantification using the operational model with Michaelis-Menten based quantification; the latter accurately quantified ligand efficacies despite large difference in ligand affinities. Together, these results showed that the V2R is promiscuous in its ability to engage several G proteins and that its signaling profile is biased by small structural changes in the ligand.

## SIGNIFICANCE STATEMENT

By modelling the G protein activation as Michaelis-Menten reaction, we developed a novel way of quantifying signalling bias. V2R activates, or at least engages, G proteins from all G protein subfamilies, including Gi2, Gz, Gq, G12, and G13. Their relative activation may explain its Gs-independent signalling.

## Introduction

G protein-coupled receptors (GPCRs) are a family of membrane proteins involved in many physiologic processes, including vision, olfaction, taste, hormone regulation, and neurotransmission. Their ligand-binding sites accessible from the extracellular milieu and their impact on intracellular signaling make them prime drug targets (Rask-Andersen et al., 2014). GPCRs translate ligand-binding events into cellular signals via activation of heterotrimeric G proteins and arrestins. Experimental evidence shows that many receptors can activate or engage more than one G protein isoform, not only within a single subfamily but also across the Gs/olf, Gi/o, Gq/11, and G12/13 subfamilies of heterotrimeric G proteins (Ashkenazi et al., 1987; Fargin et al., 1989; Cotecchia et al., 1990; Vallar et al., 1990; Van Sande

This work was supported by the Swiss National Science Foundation [Grants 135754 and 159748] to DBV; Swiss National Science Foundation Doc.Mobility P1EZP3\_165219 to FMH; and a Foundation [Grant 148431] from the Canadian Institute of Health Research (CIHR) to MB. BP was funded by a Fellowship Award from CIHR (2012 to 2015) and by a Fellowship Award from Diabetes Canada (2016 to 2018). MB holds a Canada Research chair in Signal Transduction and Molecular Pharmacology. MB is the chairman of the Scientific advisory board of Domain Therapeutics, a biotech company to which the BRET-based sensor used in the present study was licensed for commercial use. DBV is a founder of Z7 Biotech, a company specializing in early-stage drug discovery.

A preprint of this article was deposited in *bioRxiv* [<https://doi.org/10.1101/2021.01.28.427950>].

[dx.doi.org/10.1124/molpharm.122.000497](https://doi.org/10.1124/molpharm.122.000497).

**ABBREVIATIONS:** AVP, arginine vasopressin; BRET, bioluminescence resonance energy transfer; HEK, human embryonic kidney; RlucII, *Renilla reniformis* luciferase; V2R, Vasopressin V2 receptor.

et al., 1990; Crawford et al., 1992; Gudermann et al., 1992; Zhu et al., 1994; Laprairie et al., 2017). The realization that some ligands can be agonists for one pathway and antagonists for another led to the development of the concept of biased signaling (Jarpe et al., 1998; MacKinnon et al., 2001; Azzi et al., 2003; Wei et al., 2003; Galandrin et al., 2007; Kenakin and Miller, 2010). Such biased ligands are very promising pharmaceuticals because pharmacological benefits are often associated with one pathway while the side-effects are mediated by another (Bohn, et al. 1999; Bohn et al., 2000; Galandrin et al., 2007; Kenakin and Christopoulos, 2013b; Rankovic et al., 2016; Benredjem et al., 2019).

Several approaches to quantify signaling bias have been suggested (reviewed in Kenakin and Christopoulos, 2013b; Smith et al., 2018). A widely used approach is based on the Black-Leff operational model that described the ligand binding and effector output of the receptors and provided a framework for the development of quantitative pharmacology (Black and Leff, 1983). It was further developed by Kenakin and Christopoulos (Kenakin et al., 2012; Kenakin and Christopoulos, 2013a) and Rajagopal and Lefkowitz (Rajagopal et al., 2011; Rajagopal, 2013; Stahl et al., 2019). One of the important aspects of this model is its simplicity while capturing essential aspects of the signaling process. On the other hand, it is a heuristic model that links the signaling input to the signaling output without considering the underlying mechanisms.

The vasopressin V2 receptor (V2R) is a family A GPCR expressed in several tissues (Szczechanska-Sadowska et al., 2021) and is mainly known for its action in the kidney. It mediates the action of the antidiuretic hormone, arginine-vasopressin (AVP), by promoting the translocation of the water channel aquaporin to the apical membrane of the principal cell of the collecting duct, leading to water reabsorption. Although classically known as a Gs-coupled receptor, it has also been proposed to activate Gq (Zhu et al., 1994; Inoue et al., 2019) and was reported to nonproductively engage G12 (Okashah et al., 2020) and form noncanonical receptor-Gi-arrestin complexes (Smith et al., 2021). V2R is a target for treating central diabetes insipidus (Moeller et al., 2013; Qureshi et al., 2014) and polycystic kidney disease (Rinschen et al., 2014; Sparapani et al., 2021).

Here, we developed a simple Michaelis-Menten (M-M) approach for quantifying G protein activation that can better separate the effects of ligand affinity versus potency in calculating the signaling bias. This model accurately describes the behavior of G protein activation by GPCRs without the need for “functional” affinity, and instead uses  $K_d$  values measured in the ligand-binding experiment. The ligand efficacy is reflected by a single parameter, M-M  $k_{cat}$ . We show that the V2R can engage many G proteins, including members of the Gq (G $\alpha_q$ , G $\alpha_{11}$ , G $\alpha_{14}$ , and G $\alpha_{15}$ ) as well as members of the Gi (G $\alpha_{i1}$ , G $\alpha_{i2}$ , G $\alpha_{i3}$ , and G $\alpha_{z2}$ ) subfamilies. We compared signaling of four closely related natural and synthetic peptide ligands for the V2R, AVP, vasotocin, oxytocin, and desmopressin using the developed M-M model as well as the operational model for quantification of bias. Overall, the M-M model robustly reports relative changes in ligand efficacies, and these results suggest that even relatively minor structural changes in the ligand can induce significant signaling bias at the V2R. These findings open the path for discovering

biased ligands, allowing us to dissect the physiologic role of individual pathways.

## Materials and Methods

**Vasopressin V2 Receptor Ligands.** [Arg<sup>8</sup>]-Vasopressin (AVP) (Cys-Tyr-Phe-Gln-Asn-Cys-Pro-Arg-Gly-NH<sub>2</sub>; disulphide bridge: Cys<sup>1</sup>-Cys<sup>6</sup>, 1085.25 g/mol), desmopressin acetate (deamino-Cys-Tyr-Phe-Gln-Asn-Cys-Pro-D-Arg-Gly-NH<sub>2</sub>; disulphide bridge: Cys<sup>1</sup>-Cys<sup>6</sup>, 1069.24 g/mol), and oxytocin acetate (Cys-Tyr-Phe-Gln-Asn-Cys-Pro-Arg-Gly-NH<sub>2</sub>; disulphide bridge: Cys<sup>1</sup>-Cys<sup>6</sup>, 1085.25 g/mol) were purchased from Genemed Synthesis Inc. (San Antonio, TX, USA) and [Arg<sup>8</sup>]-vasotocin acetate (Cys-Tyr-Ile-Gln-Asn-Cys-Pro-Arg-Gly-NH<sub>2</sub>, disulphide bridge: Cys<sup>1</sup>-Cys<sup>6</sup>, 1050.22 g/mol) was from Sigma-Aldrich (Ontario, Canada).

**Biosensor Constructs.** Our biosensor measurements are based on BRET assay technology (Dionne et al., 2002). For the plasmids encoding for RlucII-G $\alpha$  constructs, constructs were prepared using flexible NAAIRS linkers to insert *Renilla* luciferase (RlucII) into the coding sequence of human G $\alpha$  versions. RlucII was inserted between amino acids Asp<sup>94</sup> and Phe<sup>95</sup> of G $\alpha_{zz}$  using NAAIRSTRPRCT and TRPRCTNAAIRS as linkers. The G $\alpha_{i1}$ , 2 and 3 RlucII fusions contain a duplication of the respective loop where the RlucII was inserted; namely DSA and RLKIDFG for G $\alpha_{i1}$ , ADPS, and NLQIDF for G $\alpha_{i2}$ , EAA, and RLKIDFG for G $\alpha_{i3}$ , always followed and preceded by NAAIRS, respectively. Insertion positions were Gly<sup>96</sup>/Asp<sup>97</sup> for G $\alpha_{i1}$ , Phe<sup>95</sup>/Ala<sup>96</sup> for G $\alpha_{i2}$ , and Gly<sup>96</sup>/Glu<sup>97</sup> for G $\alpha_{i3}$ . The G $\alpha_{zoA}$  construct was described previously (Richard-Lalonde et al., 2013). G $\gamma_1$ , G $\gamma_2$  and G $\gamma_5$  were N-terminally tagged with GFP10 as described (Gales et al., 2006) and  $\beta$ -arrestin 1 and 2 were N-terminally fused to RlucII (Perroy et al., 2004). In the protein kinase C (PKC) biosensor, GFP10 was followed by two phospho-sensing domains, FHA1 and FHA2, and two phospho-PKC (pPKC) sequences, the RlucII and the C1b domain from PKC $\delta$ . The pPKC sequences can be phosphorylated by natively-expressed PKC, PKC $\delta$  then binds diacylglycerol (DAG), leading to membrane recruitment (Namkung et al., 2018). Activation of the GPCR leads to activation of phospholipase C $\beta$ , followed by accumulation of DAG, which activates PKC. The PKC natively expressed in HEK293 cells phosphorylates pPKC1 and 2 domains of the PKC biosensor, which causes a conformational change and BRET increase. Through the C1b domain of PKC $\delta$ , the sensor is recruited to DAG in the plasma membrane.

**Cell Culture and Transfection.** Human embryonic kidney (HEK) 293SL cells were transiently cotransfected with Flag-V2R, different RlucII-G $\alpha$  variants, G $\beta_1$ , and GFP10-G $\gamma_1$  for G protein activation measurements and with Flag-V2R, RlucII- $\beta$ -arrestin1 or 2, and CAAX-GFP10 for  $\beta$ -arrestin recruitment measurements. For Protein kinase C (PKC) activation, HEK293  $\Delta$ Gq/11/12/13 cells were transiently cotransfected with Flag-V2R and unimolecular PKC biosensor for controls and with Flag-V2R, unimolecular PKC biosensor and either Gq, G11, G14 or G15 for activation experiments. The HEK293  $\Delta$ Gq/11/12/13 cells were obtained by CRISPR-Cas9 technology (Inoue et al., 2019). Linear 25 kDa polyethyleneimine (PEI) (Polysciences Inc.) was prepared in phosphate-buffered saline (PBS) (Multicell) (PEI:DNA ratio 3:1). Per 0.24 million HEK293SL cells, 1  $\mu$ g DNA was used. The cells were seeded into white Cellstar PS 96-well cell culture plates (Greiner Bio-One, Germany) at a density of 20,000 cells per well and grown for 48 hours at 37°C with 5% CO<sub>2</sub>.

**Biosensor Measurements.** Forty eight hours after transfection, the 96-well plates were washed with 200  $\mu$ l PBS/well and 90  $\mu$ l of Tyrode's buffer (NaCl 137 mM, KCl 0.9 mM, MgCl<sub>2</sub> 1 mM, NaHCO<sub>3</sub> 11.9 mM, NaH<sub>2</sub>PO<sub>4</sub> 3.6 mM, Hepes 25 mM, glucose 5.5 mM, CaCl<sub>2</sub> 1 mM pH 7.4) were added and the cells were stored at 37°C with 5% CO<sub>2</sub> for 2 hours before the measurement. For the measurement, the plates are incubated with 10  $\mu$ l ligand or vehicle per well for 5 minutes at varying concentrations, then 10  $\mu$ l coelenterazine 400a (also known as DeepBlueC) 2.5  $\mu$ M final were added. After further

5 minutes of incubation, luminescence and GFP10 counts were measured at 410 and 515 nm, respectively, in a Synergy Neo (Biotek) plate reader using 0.4 second integration time.

**Preparation of Ligands.** All ligands were prepared in 0.1% (w/v) BSA, stock solutions were stored at  $-20^{\circ}\text{C}$  while dilutions for the experiments were stored at  $4^{\circ}\text{C}$ . All ligand dilutions for experiments were used within 4 days of preparation.

**Michaelis-Menten Based Description of the G Protein Activation by a GPCR.** In the enzymatic model of GPCR activity, the G protein activation is catalyzed by the receptor and is dependent on the agonist binding (Waelbroeck et al., 1997; Roberts and Waelbroeck, 2004). The concentration of the active agonist-bound receptor  $R(L)$  is described by a binding isotherm:

$$R(L) = \frac{R_{\text{tot}} \cdot L}{K_d + L} \quad (1)$$

where  $R_{\text{tot}}$  is the total concentration of the receptor,  $L$  is ligand concentration, and  $K_d$  is the ligand dissociation constant.

A minimal system considers the formation of product (P, activated G protein, G $\alpha$ -GTP) as a function of agonist-bound receptor concentration  $R(L)$ , that is described by the eq. 1 above, its catalytic activity rate constant  $k_{\text{cat}}$ , as well as the Michaelis constant  $K_m$  for the G protein–receptor interaction. The rate of deactivation of the activated G protein (P) into inactive G protein (S) depends on the concentration of product and the hydrolysis rate constant  $k_h$  of GTP to GDP at the G $\alpha$  subunit.

$$\frac{d[P]}{dt} = \frac{R(L) \cdot k_{\text{cat}} \cdot [S]}{K_m + [S]} - k_h \cdot [P] \quad (2)$$

Considering the deactivation of the active G protein via GTP hydrolysis is an important feature of this model as it determines the concentration of the activated G protein.

At steady-state conditions there is an analytical solution yielding the concentration of activated G protein [P] as a function of the total (i.e. inactive and active combined) concentration of the G protein,  $S_0$ .

$$[P] = S_0$$

$$-\left(\frac{R(L)k_{\text{cat}}}{k_h} - S_0 + K_m\right) + \sqrt{\left(\frac{R(L)k_{\text{cat}}}{k_h} - S_0 + K_m\right)^2 + 4K_m S_0} \quad (3)$$

From the mathematical point of view, what matters for the steady-state solution is the apparent catalytic activity of the receptor–ligand complex in activating a G protein in a given system:

$$A_{\text{cat}} = R(L) \cdot \frac{k_{\text{cat}}}{k_h} \quad (4)$$

where  $R(L)$  and  $k_{\text{cat}}$  depend on the ligand affinity and concentration as well as the ligand signaling properties whereas  $k_h$  depends on the G protein and other system parameters.

Subsequently, the eq. 3 could be simplified to

$$[P] = S_0 - \frac{-(A_{\text{cat}} - S_0 + K_m) + \sqrt{(A_{\text{cat}} - S_0 + K_m)^2 + 4K_m S_0}}{2} \quad (5)$$

Correspondingly, the steady-state bias factor between two ligands for a given system can be expressed as

$$B_{\text{mm}} = \frac{k_{\text{cat}}(\text{ligand})}{k_{\text{cat}}(\text{reference ligand})} = \frac{A_{\text{cat}}(\text{ligand})}{A_{\text{cat}}(\text{reference ligand})} \quad (6)$$

at the concentration of the ligand that results in the same occupancy of the receptor.

Although in our experiments the values of  $S_0$  and  $K_m$  are not known, it is their value relative to the  $A_{\text{cat}}$  that would define the shape of the response curve. Therefore, for data fitting purposes we

set their values to 1 and only interpret changes relative to the reference ligand.

The concentration-response curves of biosensor responses were fitted to the following equation:

$$F(L) = \frac{F_1[P]}{S_0} + \frac{F_0(S_0 - [P])}{S_0} \quad (7)$$

Where [P] was calculated based on eq. 1 and eq. 3,  $F_0$  and  $F_1$  are the biosensor signal values in the nonactivated and activated states, respectively. The data for individual ligands were fitted simultaneously to a MM model described above using the in house DataFitter software (D. Veprintsev, <https://github.com/dbv123w/DataFitter>). A GraphPad PRISM file containing this model is available for download from [https://github.com/dbv123w/GPCR\\_MM](https://github.com/dbv123w/GPCR_MM).

**Simulations of Michaelis-Menten Based Description of the G Protein Activation by a GPCR.** All simulations were performed using Cell Designer (Funahashi et al., 2003). The value of the parameters of the system ( $R_{\text{tot}}$ ,  $k_{\text{cat}}$ ,  $k_h$ ,  $K_m$  and  $S_0$ ) were fixed to 1, whereas the value of the parameter presented on the y-axis and the ligand concentration were varied.

**Data Analysis Using Operational Model.** Data analysis was done in GraphPad Prism version 6.05 for Windows (GraphPad Software, La Jolla California USA, [www.graphpad.com](http://www.graphpad.com)). The statistical significance of G protein activation and  $\beta$ -arrestin recruitment was initially assessed by a one-sample  $t$  test compared with 0 with  $n = 3$  ( $*P < 0.05$ ,  $**P < 0.01$  and  $***P < 0.001$ ). For concentration-response curves, all data points were normalized to the maximal response obtained with AVP and expressed as percentage. Values are given  $\pm$ S.E.M for  $n$  experiments. Bias factors were calculated according to the operational model (Black and Leff, 1983). The final equation used for nonlinear curve fitting is:

$$E = \text{basal} + \frac{E_m - \text{basal}}{1 + \left(\frac{[A]}{10^{\log K_A} + 1}\right)^n} \quad (8)$$

where  $E$  is the ligand effect,  $[A]$  is the agonist concentration,  $E_m$  is the maximal response of the system, basal is the signal in absence of ligand,  $K_A$  is the functional equilibrium constant,  $R$  is the transduction coefficient  $\frac{\tau}{K_A}$  where  $\tau$  is an index for the efficacy of the agonist and  $n$  is the slope (Evans et al., 2011; Kenakin et al., 2012; Kenakin and Christopoulos, 2013b; van der Westhuizen et al., 2014).

## Results

**Analysis of the G Protein Activation Using the Michaelis-Menten Formalism.** One of the very promising approaches to describe and quantify the activity of GPCRs receptors in vivo and in vitro is by the enzymatic model (Waelbroeck et al., 1997; Roberts and Waelbroeck, 2004) and, in its simplified form, by the Michaelis-Menten formalism (Ernst et al., 2007; Maeda et al., 2014). The receptor is considered an enzyme that catalyzes the conversion of substrate to product, i.e., inactive G protein to activated G protein. Therefore, it is important to consider that the activated G protein will be deactivated by autohydrolysis of bound GTP to GDP. The use of this model allows obtaining the intrinsic enzymatic activity of the ligand-receptor complex toward a G protein that can be used for the calculations of intrinsic bias factors. To reliably fit concentration-response curves, it is essential to keep the model simple, with a minimal number of parameters. Therefore, the Michaelis-Menten formalism is preferred to the full enzymatic

model as it has the same number of parameters as the operational model.

**In Silico Analysis of the Michaelis-Menten Model of G Protein Activation.** The first parameter to consider is the concentration of available G protein ( $S_0$ ). The ability of the G protein to interact with the activated receptors is determined by the second parameter, the Michaelis constant  $K_m$ .  $K_m$  describes the concentration of G protein at which the G protein activation by the receptor is half-maximal. Third, the number of active receptors is a combination of the receptor number and activity ( $R_{tot} \cdot k_{cat}$ ). High activity can compensate for low receptor numbers and vice versa. The final parameter is  $k_h$ , the rate of hydrolysis of GTP to GDP at the G protein, which returns the G protein to its inactive state. The mathematical description of this model is included in the Methods section (eq. 1–3). To explore the model and the impact of parameters' variations, we modeled effects of receptor activity, G protein deactivation, G protein concentration, and the  $K_m$  of the G proteins toward receptor on the observed activation of the G proteins and, correspondingly, biosensor responses (Fig. 1 and 2). The system needs sufficient G protein (comparable to the  $K_m$  value or above) for the G protein activation to take place. However, further increase in the G protein concentration does not increase the potency of the response (i.e. left shift of the curve) as the response (under simulation conditions, see Methods) follows the ligand-binding curve (Fig. 2). Correspondingly,  $K_m$  should be comparable or lower than the concentration of the G protein for the activation to happen (Fig. 2). The system response is far more sensitive to changes in the catalytic activity of the activated receptor ( $k_{cat}$ ) and the rate of the G protein deactivation ( $k_h$ ) than to changes in  $K_m$  or total G protein concentration  $S_0$ . The more active the receptor is, the fewer active receptor molecules are needed to reach 50% of the response, leading to a left shift of the activation curve relative to the ligand binding. Therefore, the model captures the classic “receptor reserve” concept (Kenakin, 2014). In contrast, an increase in the rate of G protein deactivation  $k_h$  (Fig. 3) directly opposes the activity of the receptor ( $k_{cat}$ ). To test and compare our newly developed model, we evaluated the signaling of a promiscuous GPCR, the vasopressin V2 receptor, for four peptide ligands.

**Vasopressin V2 Receptor Recruits Members of all G Protein Families and Both  $\beta$ -Arrestins.** We used biosensors based on bioluminescence resonance energy transfer (BRET) to study the engagement of different G proteins. For the heterotrimer  $G\alpha\beta\gamma$  biosensor, the  $G\alpha$  subunit was tagged with luciferase (RlucII) (Gales et al., 2006; Breton et al., 2010; Schonegge et al., 2017), and the  $G\gamma$  subunit was tagged with GFP10 (Fig. 3A, Methods). We measured the ligand-mediated  $\Delta$ BRET for different  $G\alpha$  proteins. V2R was able to engage  $G\alpha_s$ ,  $G\alpha_{i1}$ ,  $G\alpha_{i2}$ ,  $G\alpha_{i3}$ ,  $G\alpha_z$ ,  $G\alpha_q$ ,  $G\alpha_{12}$  and  $G\alpha_{13}$  to different extents in response to the natural ligand, AVP, but failed to recruit or activate  $G\alpha_oA$  and  $G\alpha_oB$  (Fig. 3B). These data indicate that V2R can engage a broad panel of G protein belonging to all the subfamilies, beyond the previously reported  $G_s$  and  $G_q$  (Zhu et al., 1994; Inoue et al., 2019). To further explore V2R  $G_q$  activation, we used a protein kinase C (PKC) biosensor (Namkung et al., 2018) in  $G_q/11/12/13$  knock-out cells ( $G_q$ -KO) (Inoue et al., 2019), supplemented with the individual  $G\alpha$  subunits. This biosensor detects the phosphorylation-induced association of forkhead-associated domains selectively binding to PKC-phosphorylated sites

(Fig. 3C). Upon addition of AVP, no PKC activation could be detected in  $G_q$ -KO cells. However, significant PKC activation was observed upon complementation with  $G\alpha_q$ ,  $G\alpha_{11}$ ,  $G\alpha_{14}$ , or  $G\alpha_{15}$  (Fig. 3D). The specific activation of PKC through co-transfected  $G_q$  family members shows that V2R not only couples to but also activates all  $G_q/11$  family members. In addition, we tested G protein activation in combination with three different  $G\gamma$  subunits:  $G\gamma_1$ ,  $G\gamma_2$ , and  $G\gamma_5$  (Fig. 3E) for G proteins where we detected engagement, except for the canonically activated  $G_s$ . AVP led to a decrease in BRET signal for all the  $G\gamma$  tested for the  $G_i$  and  $G_q$  family members. For  $G_{12}$ , although a robust BRET decrease was observed with  $G\gamma_1$ , BRET signal increases were observed for  $G\gamma_2$  and  $G\gamma_5$ . This observation may indicate a difference in the interaction of V2R with  $G\alpha_{12}$  compared with other  $G\alpha$  subunits in agreement with a recent study reporting the formation of unproductive V2R- $G\alpha_{12}$  complexes (Okashah et al., 2020). For  $G_{13}$ , BRET decreases were observed for  $G\gamma_1$  and  $G\gamma_2$  but not for  $G\gamma_5$ , pointing to a different generalized type of interaction for the  $G_{12/13}$  family members. In addition, we measured  $\beta$ -arrestin recruitment using an enhanced bystander BRET (ebBRET)-based biosensor that uses RlucII- $\beta$ -arrestin 1 or 2 and a Renilla GFP (rGFP)-tagged CAAX box domain from KRas, which is inserted into the membrane (Fig. 3F) (Namkung et al., 2016). V2R recruited both  $\beta$ -arrestins to the same extent (Fig. 3G) at saturating concentrations of AVP, consistent with published data (Oakley et al., 2000).

**Slight Differences in Peptide Ligand Sequences Give Rise to Functional Selectivity.** To determine signaling bias among peptide ligands, we compared AVP to the clinically used analog desmopressin, the nonmammalian analog vasotocin, and the low potency natural agonist oxytocin. The nonpeptides contain a disulfide bridge and differ in either one or two amino acids (Fig. 4A). Desmopressin contains deamino-Cys instead of Cys at position 1 and D-Arg instead of Arg at position 8. In vasotocin, Leu is replaced with Ile at position 3, a change also found in oxytocin. In addition, oxytocin contains a Leu at position 8 instead of the Arg present in AVP. We tested the effect of these four ligands on G protein engagement, protein kinase C activation through  $G\alpha_q$  family members and  $\beta$ -arrestin 1/2 recruitment. We measured concentration-response curves to determine efficacy and potency (pEC50) (Fig. 4B). In our experiments, all ligands were full agonists or strong partial agonists for  $\beta$ -arrestin recruitment and G protein engagement (Table S1). However, the potencies (pEC50) differed by almost 2.5 orders of magnitude between AVP and oxytocin (Table 1), which agrees with previously measured radio-ligand binding data. (Chini et al., 1995) (Table 2). The efficacies and potencies of the tested ligands were similar for  $G_q$  activation tested using the PKC biosensor versus direct activation with the  $G\alpha$ - $G\gamma$  biosensor (Table 1). All the pathways followed the affinity rank order except for  $G_z$ ,  $G_{12}$ , and  $G_{13}$ . For  $G_{13}$ , AVP and desmopressin were equipotent, and for  $G_{12}$  and  $G_z$ , AVP, desmopressin and vasotocin were equipotent. In addition, oxytocin showed a preference toward G protein engagement, with a lower potency for recruitment of  $\beta$ -arrestin than for G proteins. None of the ligands showed a preference for one of the  $\beta$ -arrestins.

To quantify ligand biases, we calculated transduction coefficients ( $\log(\tau/K_A)$  values) according to the operational model of agonism (Fig. 4C) (Black and Leff, 1983; Black et al., 1985; Kenakin et al., 2012). AVP was chosen as the reference

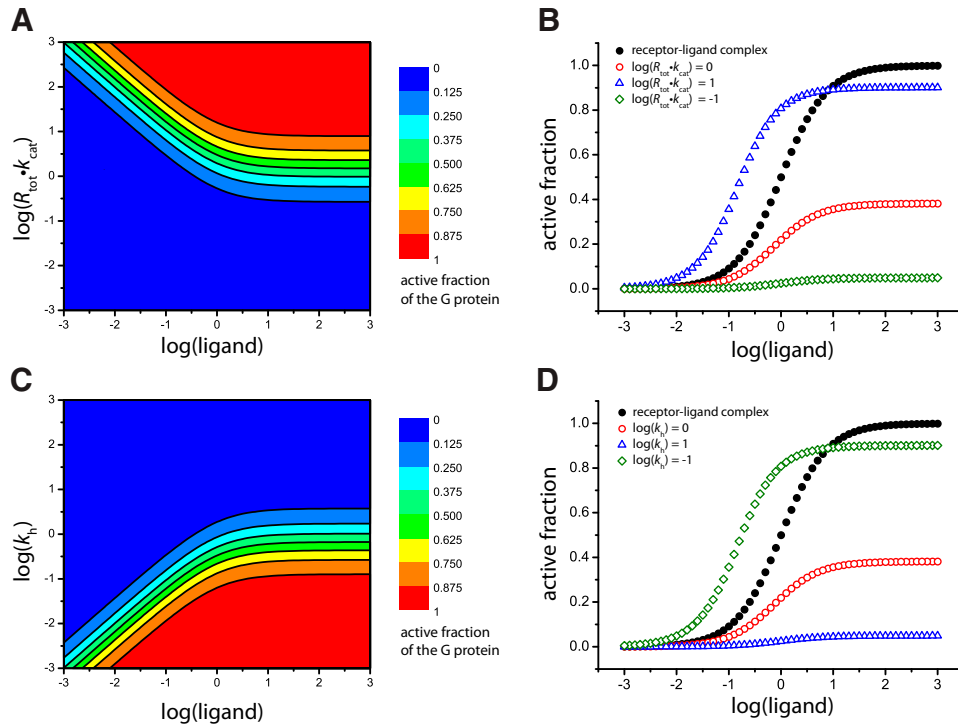


**Fig. 1.** Activation of the G protein modeled according to the Michaelis-Menten formalism so that G protein activation is half maximal and  $\log(\text{ligand}) = 0$  refers to the ligand concentration where the concentration of ligand equals  $K_A$ .  $R_{tot} \cdot k_{cat}$  was modeled as one parameter because a high receptor number ( $R_{tot}$ ) can compensate for a slow  $k_{cat}$  and vice versa. The units are arbitrary. (A) Fraction of active G protein as a function of receptor activity and amount ( $R_{tot} \cdot k_{cat}$ ). (B) examples of individual curves of (A) at several receptor activity levels. (C) Fraction of active G protein as a function of G protein deactivation rate constant  $k_h$ . (D) examples of individual curves at different  $\log(k_h)$  values. Both parameters can result in a shift of the EC50 value as well as the amplitude of the response.

agonist (Table 3). The choice of a reference agonist is necessary to eliminate observational and system bias (Kenakin and Christopoulos, 2013b). The signaling responses to desmopressin and vasotocin were reduced by a factor of 3 to 5, except for G12 and Gz. For oxytocin, the responses for all pathways, including Gz and G12, was reduced by about a factor of 100. Comparison of the ability of the V2R to activate G proteins (Fig. 4) relative to the reported affinity (Table 2) does not indicate that oxytocin is a particularly weak agonist compared with other peptides. Considering that all peptides elicited the full amplitude of the biosensor response, the  $\tau$  should be relatively large (i.e.  $> 10$ ), and the difference between the receptor-ligand complex formation and the effector activation response curve should be separated by at least a log unit (Black et al., 1985). On the other hand, the  $\Delta \log(\tau/K_A)$  values were significantly reduced for the lower-affinity ligands, implying a potential overestimation of the  $K_A$  value that reflects the affinity of the agonist for the “active” state of the receptor. Both  $\tau$  and  $K_A$  are estimated by fitting the same concentration-response curves, which significantly increases the uncertainty of their evaluation. An alternative application of the Black-Leff operational model has also been used for evaluating signaling bias (Rajagopal et al., 2011; Rajagopal, 2013), where the value of  $K_A$  is derived from ligand binding experiments. This prompted us to develop alternative metrics that would link the bias calculations to the experimentally measured ligand affinity and report changes in receptor activity toward a particular effector at an equal level of receptor saturation by the ligand.

**Application of Michaelis-Menten Model to the Experimental Data.** To apply the developed M-M model to available experimental data, further assumptions need to be made. The rate of the G protein deactivation (specific for a G protein type) is determined by the “system” (the cells used for the experiments) and can be assumed to be constant, although we anticipate the  $K_m$  values for a given effector to be affected by the ligand, it should still be comparable to the G protein concentration. It does not introduce significant error in the system. Therefore,  $k_{cat}$  is the only significant parameter that determines the system’s behavior; all other parameters can be kept constant. The values are set to one in arbitrary units for the purpose of the fit and are canceled out by normalization. Normalization of the obtained  $k_{cat}$  to that of a reference compound allows us to define a Michaelis-Menten bias factor  $B_{mm}$ , where

$$B_{mm} = k_{cat}(\text{ligand})/k_{cat}(\text{reference ligand}) \quad (9)$$

The concentration-response curves were fitted directly considering the reported  $K_d$  values (Chini et al., 1995) (see Methods). We have applied this model to the  $G\alpha\beta\gamma$  BRET-based biosensor data (Fig. 4B).

**Comparison of Michaelis-Menten and Operational Models.** The most noticeable difference to the bias factors calculated using the operational model is that the intrinsic activity and  $B_{mm}$  bias factors of oxytocin are comparable to those of other peptides (Fig. 4D). This mirrors direct observations of the oxytocin activity as presented in Fig. 4B. As the affinity of the ligand does not affect the calculated  $k_{cat}$  or  $B_{mm}$ , the differences in the efficacy of the V2R toward G

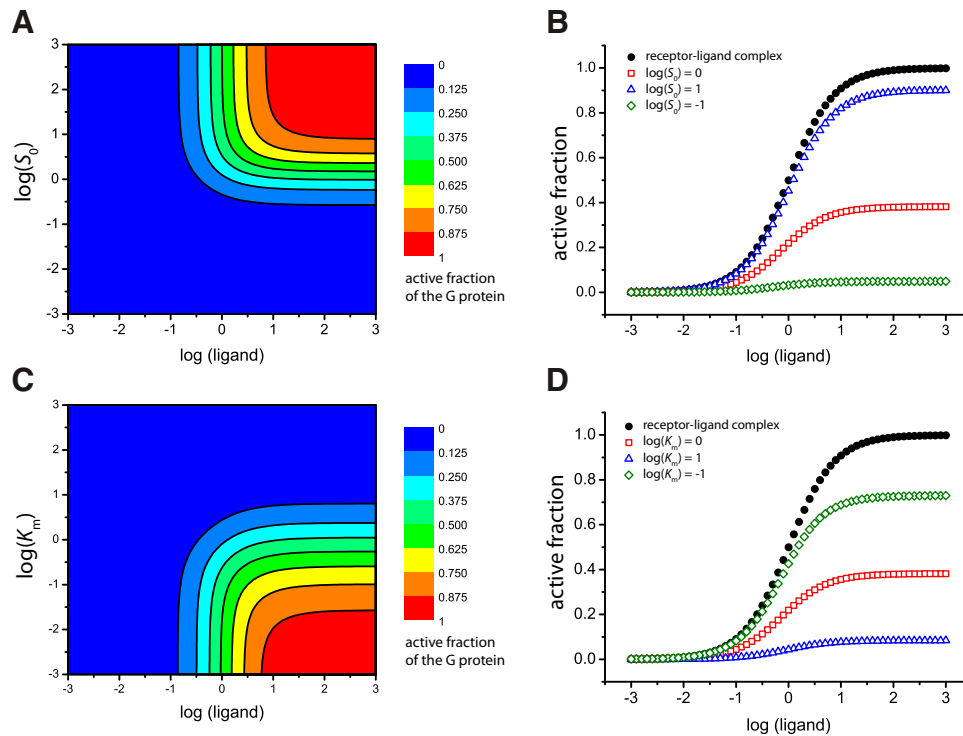


**Fig. 2.** Dependence of G protein activation on total G protein concentration  $S_0$  and the Michaelis constant  $K_m$  for G protein–receptor interaction. Either  $S_0$  or  $K_m$  was varied; the other parameters were kept constant. In addition, the ligand concentration was varied over three orders of magnitude. (A) The fraction of active G protein is shown as a function of the total amount of G protein in the system ( $S_0$ ), assuming a  $K_m$  value of 1 ( $S_0 = K_m$  at  $\log(S_0) = 0$ ). (B) Examples of individual curves at several G protein concentrations. (C) The fraction of active G protein as a function of the  $K_m$  value between the receptor and the G protein. The lower the value, the stronger the interaction. (D) Examples of the concentration-response curves normalized to the total amount of the G protein in the system. The EC50 value is not affected by these parameters, but the amplitude is.

proteins in response to binding of diverse ligands are more accentuated. Oxytocin shows a significantly reduced ability to promote V2R-mediated activation of Gs and Gi2 compared with AVP and other peptides. Compared with AVP, all tested peptides have an increased ability to promote G12 engagement but reduced ability to activate Gq. This parallels the analysis done using the operational model (Table 4). The results strongly suggest that ligands can readily bias V2R signaling, and even relatively small structural differences in peptide ligand sequence seem to be sufficient to induce this effect.

## Discussion

**Michaelis-Menten Quantification of Receptor Activity.** Previous work has shown the applicability of the enzymatic model of GPCR activity (Waelbroeck et al., 1997; Roberts and Waelbroeck, 2004). Kenakin and Christopoulos have commented on the apparent similarity between the operational model and the Michaelis-Menten equation (Kenakin and Christopoulos, 2013a). However, despite the apparent mathematical similarity, the actual solution for the steady-state concentration of activated G protein is rather different (see Methods). Here we showed that M-M model describes the activation of G proteins as a function of ligand concentration rather well. The reported efficacy parameter  $k_{cat}$  has the same meaning as  $\tau$  in the operational model, and the ratio of these parameters for two ligands activating the same pathway is a measure of ligand bias. The use of the

experimentally reported ligand affinity simplifies the analysis and improves the robustness of the  $k_{cat}$  estimation from the concentration-response curves.

It should also be noted that the simplified Michaelis-Menten model presented here can describe G protein activation but not  $\beta$ -arrestin recruitment because of the underlying nature of the two processes. First, it assumes that the number of receptor molecules is small compared with the number of G protein molecules. For most receptors, even in the over-expressed systems, this condition is very likely to be satisfied. Secondly, it also assumes that the activation of the G proteins is nonreversible during the enzymatic step. Given the very high affinity of GTP for the G protein compared with GDP while their concentrations are comparable (0.1–0.5 mM) (Traut, 1994) and the slow hydrolysis-driven deactivation of G proteins, this condition is also very likely to be satisfied. Although RGS proteins may control the rate of GTP hydrolysis of Gi and Gq proteins, they only interact with active forms of G $\alpha$  subunits after they have dissociated from G $\beta\gamma$  after the activation step (Tesmer, 2009). Thirdly, it is important to consider the differences between the signals reported by the G protein, PKC, and arrestin biosensors. Whereas G proteins are activated directly by the receptors, PKC is activated by several nested enzymatic cycles, requiring a much more complicated model incorporating several Michaelis-Menten reactions.

Arrestin biosensors report the formation of the receptor-arrestin complex with a 1:1 stoichiometry. Since this is a binding rather than an enzymatic event, it would not be

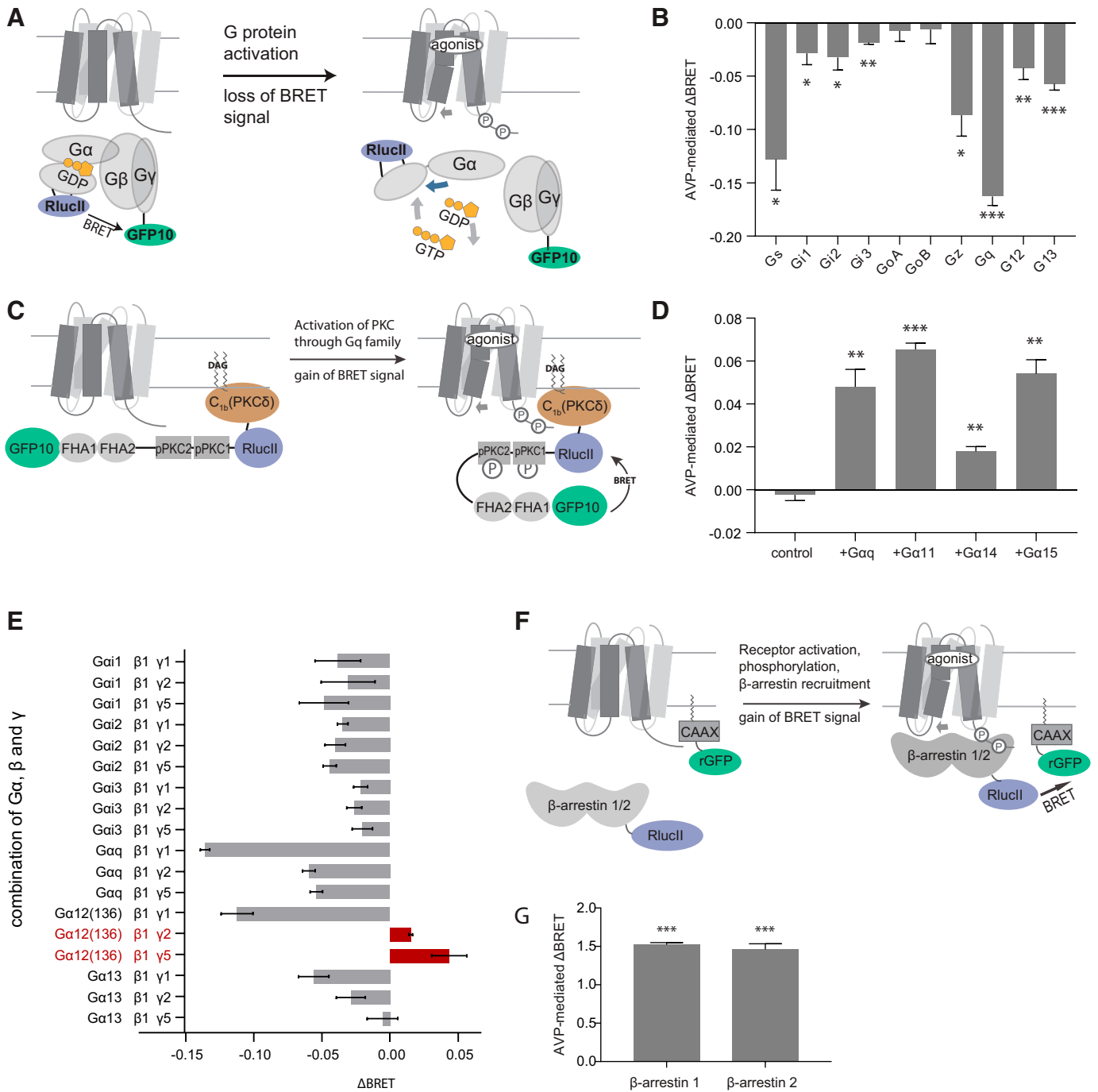


**Fig. 3.** Vasopressin V2 receptor activates  $G_s$ /olf,  $G_i$ /o,  $G_q$ /11 and  $G_{12/13}$  family proteins and both  $\beta$ -arrestins. (A) Schematic overview of the direct G protein BRET-based biosensor. Activation of the heterotrimeric G protein by the GPCR leads to dissociation of the  $G_\alpha$  from  $G\beta\gamma$  and a conformational change in the  $G_\alpha$  domain, which result in a decreased BRET signal. (B) Overview of the arginine-vasopressin (AVP)-induced change in BRET signal for RlucII-tagged  $G_\alpha$  subunits and GFP10-tagged  $G_\gamma$ 1. (C) Schematic overview of the protein kinase C (PKC) biosensor. GFP10 is followed by two phospho-sensing domains, FHA1 and FHA2 and two phospho-PKC (pPKC) sequences, which can be phosphorylated by natively-expressed PKC, the RlucII and the C1b domain from PKC $\delta$  which binds diacylglycerol (DAG), leading to membrane recruitment. Activation of the GPCR leads to activation of phospholipase C $\beta$ , followed by accumulation of DAG which activates PKC. The PKC natively expressed in HEK293 cells phosphorylates pPKC1 and 2 domains of the PKC biosensor, which causes a conformational change and BRET increase. Through the C1b domain of PKC $\delta$ , the sensor is recruited to DAG in the plasma membrane. (D) Overview of the AVP-induced change in BRET signal for the PKC biosensor when different isoforms from the  $G_q$ /11 family are cotransfected in  $G_q$ /11/12/13 null HEK293 cells. (E) G protein engagement at saturating AVP concentrations varies with  $G_\gamma$  subunit. Different combinations of  $G_\alpha$  and  $G_\gamma$  lead to differing  $\Delta$ BRET values, numbers in brackets indicate the amino acid where RlucII was fused to  $G_\alpha$ . For  $G_\alpha$ s, the alternative fusion position after amino acid 67 was used here. (F) Schematic overview of the  $\beta$ -arrestin recruitment biosensor. Activation of the GPCR leads to phosphorylation of the C-terminus of the receptor followed by recruitment of  $\beta$ -arrestin. (G) Overview of the AVP-induced change in BRET signal for RlucII-tagged  $\beta$ -arrestins and rGFP-tagged CAAX domain of Kras. The statistical significance was assessed by a one-sample  $t$  test compared with 0 with  $n = 3$  (\* $P < 0.05$ , \*\* $P < 0.01$  and \*\*\* $P < 0.001$ ). Error bars are shown as standard error of mean (SEM).

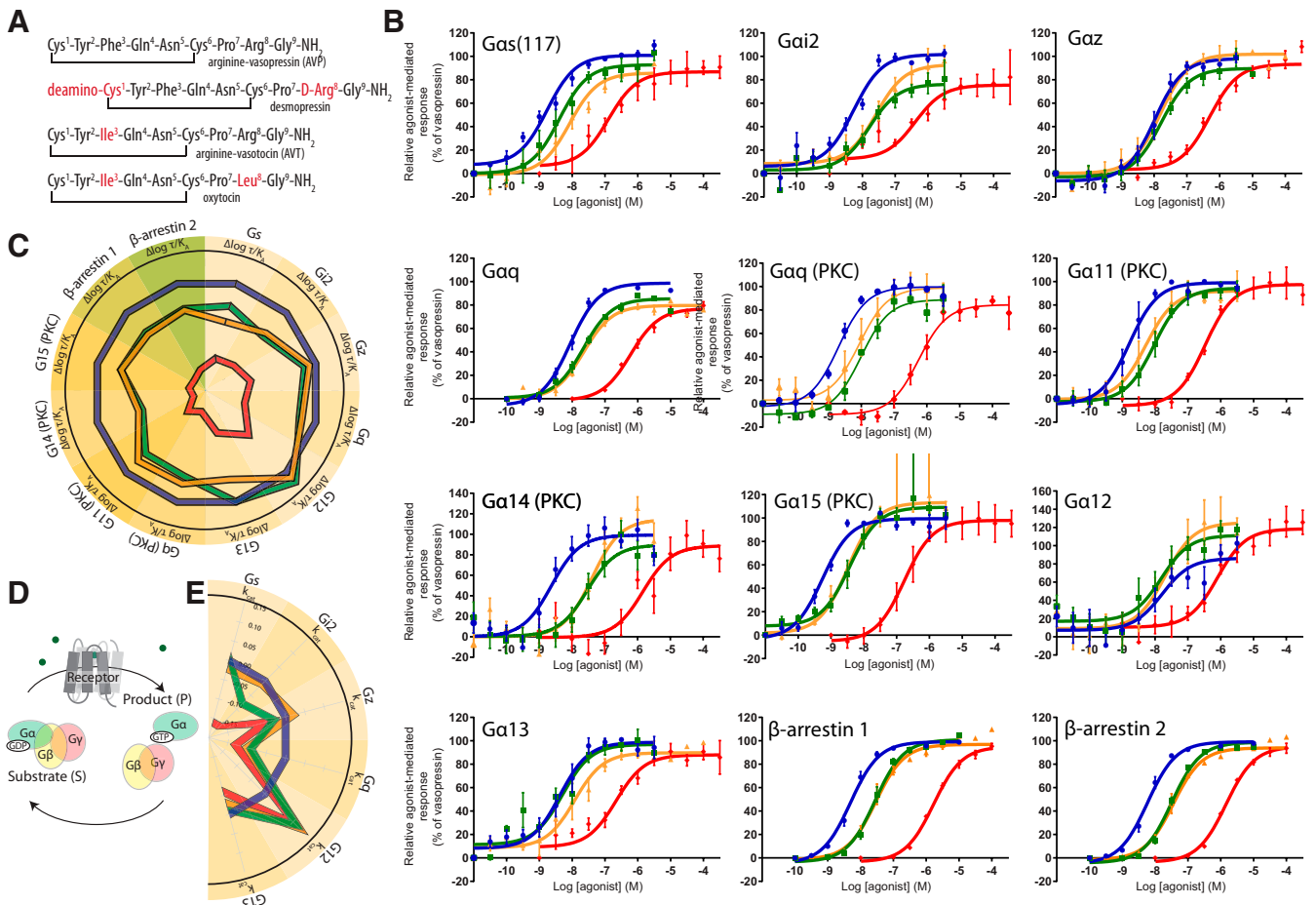


**Fig. 4.** Biased signaling of V2R peptide ligands. (A) The peptide ligands differ in only one or two amino acids (marked in red). (B) Concentration-response curves of biosensor activation for all four peptides, using the heterotrimeric  $G\alpha\beta\gamma$  biosensor for G protein engagement, the bystander-BRET  $\beta$ -arrestin biosensor for arrestin recruitment and the PKC biosensor for Gq family activation, labeled “(PKC)”. (C) Bias as calculated using the operational model for arginine vasopressin (AVP, blue), desmopressin (green), arginine vasotocin (yellow) and oxytocin (red). (D) The schematic diagram of the Michaelis-Menten model of G protein activation. (E) The Michaelis-Menten signaling bias. Although the G12 data can be fitted to a M-M model to obtain an apparent  $k_{cat}$ , additional judgement needs to be used to check if this model is applicable.

appropriate to analyze the results obtained with these arrestin-recruitment biosensors using Michaelis-Menten formalism. Recent reports suggested that arrestins may be activated and dissociate from the receptors while maintaining the active state

(Eichel et al., 2018). If this is indeed the case, it may be possible to extend the use of this model to arrestins. However, different biosensors directly reporting on the activation status of arrestin would have to be used (Charest

TABLE 1

Potencies (pEC50) and agonist-induced maximal response (“amplitude”) of G protein, protein kinase C and  $\beta$ -arrestin activation, normalized to the maximal response of Gs  
 Data are mean  $\pm$  S.E.M of 2 to 7 independent experiments done either in triplicates or quadruplicates, see details in Supplemental Table 1. Numbers in brackets indicate the fusion site of the luciferase in cases where different sensors were used.

Pathway	AVP		Desmopressin		Vasotocin		Oxytocin	
	pEC50	Response	pEC50	Response	pEC50	Response	pEC50	Response
Gs (117)	8.76 $\pm$ 0.08	100.9 $\pm$ 2.2	8.39 $\pm$ 0.14	92.8 $\pm$ 4.3	8.08 $\pm$ 0.11	85.8 $\pm$ 3.4	6.89 $\pm$ 0.16	86.8 $\pm$ 3.6
Gi2	8.27 $\pm$ 0.08	101.6 $\pm$ 2.8	7.78 $\pm$ 0.14	76.3 $\pm$ 4.0	7.58 $\pm$ 0.17	93.0 $\pm$ 5.8	6.39 $\pm$ 0.18	75.5 $\pm$ 3.9
Gz	7.98 $\pm$ 0.09	98.1 $\pm$ 3.7	7.78 $\pm$ 0.09	89.7 $\pm$ 3.3	7.81 $\pm$ 0.10	101.9 $\pm$ 3.5	6.31 $\pm$ 0.09	93.4 $\pm$ 2.8
Gq	8.07 $\pm$ 0.06	98.7 $\pm$ 2.5	7.66 $\pm$ 0.06	85.5 $\pm$ 1.9	7.65 $\pm$ 0.06	79.7 $\pm$ 1.7	6.22 $\pm$ 0.07	77.0 $\pm$ 1.9
G12	7.79 $\pm$ 0.21	86.2 $\pm$ 7.2	7.81 $\pm$ 0.25	111.4 $\pm$ 9.2	7.69 $\pm$ 0.22	125.2 $\pm$ 10.7	6.10 $\pm$ 0.16	118.5 $\pm$ 6.4
G13	8.37 $\pm$ 0.12	98.7 $\pm$ 3.8	8.32 $\pm$ 0.13	95.7 $\pm$ 3.7	7.92 $\pm$ 0.15	89.8 $\pm$ 4.1	6.66 $\pm$ 0.11	88.0 $\pm$ 2.7
PKC (Gq)	8.69 $\pm$ 0.07	99.7 $\pm$ 2.3	8.01 $\pm$ 0.10	88.8 $\pm$ 3.4	8.06 $\pm$ 0.16	98.9 $\pm$ 5.5	6.25 $\pm$ 0.11	84.4 $\pm$ 3.6
PKC (G11)	8.79 $\pm$ 0.09	99.1 $\pm$ 2.9	8.03 $\pm$ 0.09	94.4 $\pm$ 3.2	8.28 $\pm$ 0.12	92.1 $\pm$ 3.8	6.48 $\pm$ 0.09	97.5 $\pm$ 3.0
PKC (G14)	8.63 $\pm$ 0.19	97.3 $\pm$ 6.6	7.50 $\pm$ 0.43	79.4 $\pm$ 18.6	7.38 $\pm$ 0.24	142.6 $\pm$ 14.0	5.83 $\pm$ 0.25	96.2 $\pm$ 9.6
PKC (G15)	9.26 $\pm$ 0.08	99.5 $\pm$ 2.2	8.43 $\pm$ 0.1	109.2 $\pm$ 3.2	8.49 $\pm$ 0.09	113.2 $\pm$ 3.3	6.77 $\pm$ 0.14	98.1 $\pm$ 4.4
$\beta$ -arrestin 1	8.31 $\pm$ 0.05	99.2 $\pm$ 1.9	7.56 $\pm$ 0.05	101.0 $\pm$ 2.3	7.54 $\pm$ 0.06	96.9 $\pm$ 2.2	5.77 $\pm$ 0.04	95.0 $\pm$ 1.6
$\beta$ -arrestin 2	8.23 $\pm$ 0.05	99.1 $\pm$ 2.0	7.50 $\pm$ 0.04	98.8 $\pm$ 1.7	7.45 $\pm$ 0.05	93.9 $\pm$ 1.8	5.84 $\pm$ 0.04	95.1 $\pm$ 1.7

TABLE 2

Dependence of  $\log B_{mm}$  values on ligand amino-acid sequence, using AVP as the reference peptide

	AVP	Desmopressin	Vasotocin	Oxytocin
Deamination	0	1	0	0
F3L	0	0	1	1
R8L	0	0	0	1
R(L)8R(D)	0	1	0	0
$\log Ki$ (Chini et al., 1995)	-8.97	-7.51	-7.6	-5.81
Gs(67) $\log B_{mm}$	0	-0.01	-0.02	-0.17
Gs(117) $\log B_{mm}$	0	0.01	-0.02	-0.16
Gi2 $\log B_{mm}$	0	-0.08	-0.01	-0.16
Gz $\log B_{mm}$	0	-0.03	0.02	-0.05
Gz $\log B_{mm}$	0	-0.09	-0.10	-0.13
G12 $\log B_{mm}$	0	0.11	0.12	0.11
G13 $\log B_{mm}$	0	-0.01	-0.03	-0.06

F3L, exchange of a phenylalanine at position 3 for a leucine; R8L, exchange of an arginine at position 8 for a leucine; R(L)8R(D), exchange of the L- for D-arginine at position 8.

et al., 2005; Zimmerman et al., 2012; Lee et al., 2016; Nuber et al., 2016). One of the important advantages of the Michaelis-Menten formalism presented here is that it can be extended to describe the kinetics of signaling processes and not only the steady-state equilibria. The appreciation that signaling may not be an equilibrium process and the importance of considering the kinetics in quantifying bias is growing (Klein Herenbrink et al., 2016). We expect that the application of Michaelis-Menten formalism would be of great advantage in kinetic bias quantification, to study how signaling bias may affect acute, short term signaling events (e.g. cAMP concentration) versus long term (e.g. changes in gene transcription) effects of GPCR activation.

**V2R Promiscuity.** We observed that the V2R promiscuously engaged G proteins from all subfamilies. Although Gs and Gq coupling was previously discussed (Zhu et al., 1994; Inoue et al., 2019) and nonproductive G12 engagement was recently described, Gi coupling has only been implied in previous studies (Okashah et al., 2020). Our PKC activation data point toward the activation of Gq by the V2R. All other G proteins (Gi2, Gz, G12, and G13) were at least engaged.

The biologic significance of this promiscuity of engagement is beyond the scope of the present study. According to the Protein Atlas ([www.proteinatlas.org](http://www.proteinatlas.org)) (Uhlen et al., 2015), V2R is expressed in practically all tissues, except for the brain and the liver. Most G $\alpha$  isoforms are also expressed in

all tissues. Therefore, V2R can interact with all G proteins in native tissues, suggesting that its promiscuity may be biologically relevant. Dual Gs/Gi coupling has been reported for other receptors such as the  $\beta$ 2- and the  $\beta$ 1-adrenergic receptors (Xiao et al., 1995; Lukashova et al., 2020); one possible rationale for activation of both Gs and Gi/o proteins is to fine-tune the cAMP response (Stefan et al., 2011). However, this does not account for the activation of Gq/11 and recruitment of G12/13 families. Another possibility is that the biologic process triggered by the V2R may have to be mediated by a combination of signaling pathways. Recent medium- and large-scale profiling experiments confirmed that promiscuity is relatively common among GPCRs (Inoue et al., 2019; Okashah et al., 2019; Avet et al., 2022).

**Ligand-Induced Signaling Bias.** Both the affinity of peptides for V2R and their signaling properties are affected by amino acid substitutions (Table 2). Any modification of AVP testing resulted in decreased ability to activate Gq and increased ability to engage G12 (Supplemental Fig. 1). Oxytocin's double substitution reduced the ability of V2R to engage Gs and Gi proteins relative to the other G protein subtypes engaged by the receptor.

Similarly, the substitution of the L-Arg for D-Arg in desmopressin may be responsible for the reduced Gi/Gq engagement. This suggests that there are signaling bias hotspots in the ligand-binding pocket. Similar observations were reported for oxytocin receptors where slight oxytocin

TABLE 3

Transduction coefficients ( $\log(\tau/K_A)$ ) and  $\Delta\log(\tau/K_A)$  with AVP as reference ligandData are mean  $\pm$  S.E.M of 2 to 7 independent experiments done either in triplicates or quadruplicates.

Pathway	AVP	Desmopressin		Vasotocin		Oxytocin	
	$\log(\tau/K_A)$	$\log(\tau/K_A)$	$\Delta\log(\tau/K_A)$	$\log(\tau/K_A)$	$\Delta\log(\tau/K_A)$	$\log(\tau/K_A)$	$\Delta\log(\tau/K_A)$
Gs (67)	8.49 $\pm$ 0.20	8.82 $\pm$ 0.2	0.33 $\pm$ 0.28	8.04 $\pm$ 0.21	-0.45 $\pm$ 0.29	6.92 $\pm$ 0.22	-1.57 $\pm$ 0.30
Gs (117)	8.81 $\pm$ 0.11	8.20 $\pm$ 0.11	-0.61 $\pm$ 0.15	7.76 $\pm$ 0.11	-1.05 $\pm$ 0.16	6.76 $\pm$ 0.13	-2.06 $\pm$ 0.17
Gi2	8.30 $\pm$ 0.14	7.43 $\pm$ 0.17	-0.87 $\pm$ 0.22	7.54 $\pm$ 0.14	-0.76 $\pm$ 0.20	6.33 $\pm$ 0.21	-1.97 $\pm$ 0.25
Gz	7.97 $\pm$ 0.11	7.67 $\pm$ 0.11	-0.30 $\pm$ 0.16	7.80 $\pm$ 0.09	-0.18 $\pm$ 0.14	6.18 $\pm$ 0.11	-1.79 $\pm$ 0.15
Gq	8.04 $\pm$ 0.04	7.59 $\pm$ 0.06	-0.45 $\pm$ 0.07	7.66 $\pm$ 0.10	-0.38 $\pm$ 0.11	6.09 $\pm$ 0.08	-1.95 $\pm$ 0.11
G12	7.54 $\pm$ 0.25	7.88 $\pm$ 0.20	0.34 $\pm$ 0.32	7.74 $\pm$ 0.22	0.20 $\pm$ 0.33	6.12 $\pm$ 0.18	-1.42 $\pm$ 0.31
G13	8.57 $\pm$ 0.11	8.56 $\pm$ 0.12	-0.01 $\pm$ 0.16	7.95 $\pm$ 0.12	-0.62 $\pm$ 0.16	6.67 $\pm$ 0.12	-1.90 $\pm$ 0.16
PKC (Gq)	8.68 $\pm$ 0.08	7.97 $\pm$ 0.11	-0.71 $\pm$ 0.13	8.18 $\pm$ 0.10	-0.50 $\pm$ 0.12	6.19 $\pm$ 0.12	-2.49 $\pm$ 0.14
PKC (G11)	8.75 $\pm$ 0.07	8.04 $\pm$ 0.08	-0.71 $\pm$ 0.11	8.32 $\pm$ 0.09	-0.44 $\pm$ 0.11	6.44 $\pm$ 0.08	-2.32 $\pm$ 0.11
PKC (G14)	8.65 $\pm$ 0.33	7.41 $\pm$ 0.43	-1.24 $\pm$ 0.54	7.51 $\pm$ 0.15	-1.14 $\pm$ 0.36	6.01 $\pm$ 0.36	-2.64 $\pm$ 0.49
PKC (G15)	9.16 $\pm$ 0.10	8.52 $\pm$ 0.09	-0.65 $\pm$ 0.13	8.51 $\pm$ 0.09	-0.65 $\pm$ 0.13	6.64 $\pm$ 0.10	-2.53 $\pm$ 0.14
$\beta$ -arrestin 1	8.30 $\pm$ 0.05	7.58 $\pm$ 0.05	-0.72 $\pm$ 0.07	7.50 $\pm$ 0.05	-0.80 $\pm$ 0.07	5.76 $\pm$ 0.05	-2.54 $\pm$ 0.07
$\beta$ -arrestin 2	8.22 $\pm$ 0.03	7.52 $\pm$ 0.04	-0.69 $\pm$ 0.05	7.49 $\pm$ 0.05	-0.73 $\pm$ 0.05	5.85 $\pm$ 0.04	-2.37 $\pm$ 0.05

TABLE 4  
Comparison of bias between pathways with Gs as a reference ( $\Delta\Delta\log[\tau/K_A]$  values) and bias factors

Pathway	Desmopressin		Vasotocin		Oxytocin	
	$\Delta\Delta\log(\tau/K_A)$	Bias Factor	$\Delta\Delta\log(\tau/K_A)$	Bias Factor	$\Delta\Delta\log(\tau/K_A)$	Bias Factor
Gi2	$-0.26 \pm 0.27$	0.55	$0.28 \pm 0.26$	1.93	$0.08 \pm 0.31$	1.21
Gz	$0.32 \pm 0.22$	2.07	$0.87 \pm 0.21$	7.46	$0.27 \pm 0.23$	1.86
Gq	$0.17 \pm 0.17$	1.47	$0.67 \pm 0.19$	4.69	$0.11 \pm 0.21$	1.28
G12	$0.96 \pm 0.36$	9.06	$1.25 \pm 0.37$	17.58	$0.64 \pm 0.35$	4.33
G13	$0.60 \pm 0.22$	3.99	$0.43 \pm 0.23$	2.69	$0.16 \pm 0.24$	1.44
PKC (Gq)	$-0.09 \pm 0.20$	0.80	$0.55 \pm 0.20$	3.52	$-0.43 \pm 0.22$	0.37
PKC (G11)	$-0.10 \pm 0.19$	0.79	$0.61 \pm 0.19$	4.09	$-0.26 \pm 0.20$	0.55
PKC (G14)	$-0.63 \pm 0.56$	0.24	$-0.09 \pm 0.40$	0.81	$-0.59 \pm 0.52$	0.26
PKC (G15)	$-0.03 \pm 0.20$	0.93	$0.39 \pm 0.10$	2.48	$-0.47 \pm 0.22$	0.34
$\beta$ -arrestin 1	$-0.11 \pm 0.17$	0.78	$0.25 \pm 0.17$	1.76	$-0.48 \pm 0.18$	0.33
$\beta$ -arrestin 2	$-0.08 \pm 0.16$	0.84	$0.32 \pm 0.17$	2.09	$-0.31 \pm 0.18$	0.49

peptide modifications resulted in different signaling preferences (Busnelli et al., 2012). The peptide ligands of angiotensin receptor and chemokine receptors are another example (Wei et al., 2003; Ahn et al., 2004; Namkung et al., 2018) (reviewed in Steen et al., 2014). It is tempting to speculate that receptor-peptide pairs may have coevolved as a mechanism to change the activity of ancestral receptors.

## Conclusions

The proposed Michaelis-Menten approach can be readily applied to existing concentration-response curves and provides robust estimates of intrinsic ligand efficacy. Its application can help to deconvolute functional differences between ligands and contribute to drug development. We hope it will become a valuable analysis approach in the toolbox of modern pharmacology.

### Acknowledgments

The authors thank Steven Charlton and Nicholas Holliday for valuable discussions.

### Authorship Contributions

*Conducted experiments:* Heydenreich, Plouffe, Zhou, Breton, Le Gouill.

*Contributed new reagents or analytic tools:* Rizk, Inoue, Bouvier, Veprintsev.

*Performed data analysis:* Heydenreich, Plouffe, Rizk, Veprintsev.

*Wrote or contributed to the writing of the manuscript:* Heydenreich, Plouffe, Milić, Bouvier, Veprintsev.

### References

Ahn S, Shenoy SK, Wei H, and Lefkowitz RJ (2004) Differential kinetic and spatial patterns of beta-arrestin and G protein-mediated ERK activation by the angiotensin II receptor. *J Biol Chem* **279**:35518–35525.

Ashkenazi A, Winslow JW, Peralta EG, Peterson GL, Schimerlik MI, Capon DJ, and Ramachandran J (1987) An M2 muscarinic receptor subtype coupled to both adenylyl cyclase and phosphoinositide turnover. *Science* **238**:672–675.

Avet C, Mancini A, Breton B, Le Gouill C, Hauser AS, Normand C, Kobayashi H, Gross F, Hogue M, Lukasheva V et al. (2022) Effector membrane translocation biosensors reveal G protein and  $\beta$ arrestin coupling profiles of 100 therapeutically relevant GPCRs. *eLife* **11**:e74101.

Azzi M, Charest PG, Angers S, Rousseau G, Kohout T, Bouvier M, and Piñeyro G (2003) Beta-arrestin-mediated activation of MAPK by inverse agonists reveals distinct active conformations for G protein-coupled receptors. *Proc Natl Acad Sci USA* **100**:11406–11411.

Benredjem B, Gallion J, Pelletier D, Dallaire P, Charbonneau J, Cawkill D, Nagi K, Gosink M, Lukasheva V, Jenkinson S et al. (2019) Exploring use of unsupervised clustering to associate signaling profiles of GPCR ligands to clinical response. *Nat Commun* **10**:4075.

Black JW and Leff P (1983) Operational models of pharmacological agonism. *Proc R Soc Lond B Biol Sci* **220**:141–162.

Black JW, Leff P, Shankley NP, and Wood J (1985) An operational model of pharmacological agonism: the effect of E/[A] curve shape on agonist dissociation constant estimation. *Br J Pharmacol* **84**:561–571.

Bohn LM, Lefkowitz RJ, Gainetdinov RR, Peppel K, Caron MG, and Lin FT (1999) Enhanced morphine analgesia in mice lacking beta-arrestin 2. *Science* **286**:2495–2498.

Bohn LM, Gainetdinov RR, Lin FT, Lefkowitz RJ, and Caron MG (2000) Mu-opioid receptor desensitization by beta-arrestin-2 determines morphine tolerance but not dependence. *Nature* **408**:720–723.

Breton B, Sauvageau É, Zhou J, Bonin H, Le Gouill C, and Bouvier M (2010) Multiplexing of multicolor bioluminescence resonance energy transfer. *Biophys J* **99**:4037–4046.

Busnelli M, Saulière A, Manning M, Bouvier M, Galés C, and Chini B (2012) Functional selective oxytocin-derived agonists discriminate between individual G protein family subtypes. *J Biol Chem* **287**:3617–3629.

Charest PG, Terrillon S, and Bouvier M (2005) Monitoring agonist-promoted conformational changes of beta-arrestin in living cells by intramolecular BRET. *EMBO Rep* **6**:334–340.

Chini B, Mouillac B, Ala Y, Balestre MN, Trumpp-Kallmeyer S, Hoflack J, Elands J, Hibert M, Manning M, Jard S et al. (1995) Tyr115 is the key residue for determining agonist selectivity in the V1a vasopressin receptor. *EMBO J* **14**:2176–2182.

Cotecchia S, Kobilka BK, Daniel KW, Nolan RD, Lapetina EY, Caron MG, Lefkowitz RJ, and Regan JW (1990) Multiple second messenger pathways of alpha-adrenergic receptor subtypes expressed in eukaryotic cells. *J Biol Chem* **265**:63–69.

Crawford KW, Frey EA, and Cote TE (1992) Angiotensin II receptor recognized by DuP753 regulates two distinct guanine nucleotide-binding protein signaling pathways. *Mol Pharmacol* **41**:154–162.

Dionne P, Caron M, Labonté A, Carter-Allen K, Houle B, Joly E, Taylor SC and L. M (2002) BRET2: efficient energy transfer from Renilla luciferase to GFP2 to measure protein-protein interactions and intracellular signaling events in live cells, in *Luminescence Biotechnology: Instruments and Applications* (van Dyke K, van Dyke C and Woodfork K eds) pp 539–555, CRC Press, Boca Raton, FL.

Eichel K, Jullié D, Barsi-Rhyme B, Latorraca NR, Masurel M, Sibarita J-B, Dror RO, and von Zastrow M (2018) Catalytic activation of  $\beta$ -arrestin by GPCRs. *Nature* **557**:381–386.

Ernst OP, Gramse V, Kolbe M, Hofmann KP, and Heck M (2007) Monomeric G protein-coupled receptor rhodopsin in solution activates its G protein transducin at the diffusion limit. *Proc Natl Acad Sci USA* **104**:10859–10864.

Evans BA, Broxton N, Merlin J, Sato M, Hutchinson DS, Christopoulos A, and Summers RJ (2011) Quantification of functional selectivity at the human  $\alpha$ (1A)-adrenoceptor. *Mol Pharmacol* **79**:298–307.

Fargin A, Raymond JR, Regan JW, Cotecchia S, Lefkowitz RJ, and Caron MG (1989) Effector coupling mechanisms of the cloned 5-HT1A receptor. *J Biol Chem* **264**:14848–14852.

Funahashi A, Morohashi M, Kitano H, and Tanimura N (2003) CellDesigner: a process diagram editor for gene-regulatory and biochemical networks. *BIOSILICO* **1**:159–162.

Galandrin S, Oligny-Longpré G, and Bouvier M (2007) The evasive nature of drug efficacy: implications for drug discovery. *Trends Pharmacol Sci* **28**:423–430.

Galés C, Van Durm JJ, Schaak S, Pontier S, Percherancier Y, Audet M, Paris H, and Bouvier M (2006) Probing the activation-promoted structural rearrangements in preassembled receptor-G protein complexes. *Nat Struct Mol Biol* **13**:778–786.

Gudermann T, Birnbaumer M, and Birnbaumer L (1992) Evidence for dual coupling of the murine luteinizing hormone receptor to adenylyl cyclase and phosphoinositide breakdown and Ca<sup>2+</sup> mobilization. Studies with the cloned murine luteinizing hormone receptor expressed in L cells. *J Biol Chem* **267**:4479–4488.

Inoue A, Raimondi F, Kadij FMN, Singh G, Kishi T, Uwamizu A, Ono Y, Shinjo Y, Ishida S, Arang N et al. (2019) Illuminating G-protein-coupling selectivity of GPCRs. *Cell* **177**:1933–1947.e25.

Jarpe MB, Knall C, Mitchell FM, Buhl AM, Duzic E, and Johnson GL (1998) [D-Arg1,D-Phe5,D-Trp7,9,Leu11]substance P acts as a biased agonist toward neuropeptide and chemokine receptors. *J Biol Chem* **273**:3097–3104.

Kenakin T and Christopoulos A (2013a) Measurements of ligand bias and functional affinity. *Nat Rev Drug Discov* **12**:483.

Kenakin T and Christopoulos A (2013b) Signalling bias in new drug discovery: detection, quantification and therapeutic impact. *Nat Rev Drug Discov* **12**:205–216.

- Kenakin T and Miller LJ (2010) Seven transmembrane receptors as shapeshifting proteins: the impact of allosteric modulation and functional selectivity on new drug discovery. *Pharmacol Rev* **62**:265–304.
- Kenakin T, Watson C, Muniz-Medina V, Christopoulos A, and Novick S (2012) A simple method for quantifying functional selectivity and agonist bias. *ACS Chem Neurosci* **3**:193–203.
- Kenakin TP (2014) *A Pharmacology Primer: Techniques for More Effective and Strategic Drug Discovery*, fourth edition. ed. Elsevier Academic Press, Amsterdam; Boston.
- Klein Herenbrink C, Sykes DA, Donthamsetti P, Canals M, Coudrat T, Shonberg J, Scammells PJ, Capuano B, Sexton PM, Charlton SJ et al. (2016) The role of kinetic context in apparent biased agonism at GPCRs. *Nat Commun* **7**:10842.
- Laprairie RB, Stahl EL, and Bohn LM (2017) Approaches to assess biased signaling at the CB1R receptor. *Methods Enzymol* **593**:259–279.
- Lee MH, Appleton KM, Strungs EG, Kwon JY, Morinelli TA, Peterson YK, Laporte SA, and Luttrell LM (2016) The conformational signature of  $\beta$ -arrestin2 predicts its trafficking and signalling functions. *Nature* **531**:665–668.
- Lukasheva V, Devost D, Le Gouill C, Namkung Y, Martin RD, Longpré J-M, Amraei M, Shinjo Y, Hogue M, Lagacé M et al. (2020) Signal profiling of the  $\beta_1$ AR reveals coupling to novel signalling pathways and distinct phenotypic responses mediated by  $\beta_1$ AR and  $\beta_2$ AR. *Sci Rep* **10**:8779.
- MacKinnon AC, Waters C, Jodrell D, Haslett C, and Sethi T (2001) Bombesin and substance P analogues differentially regulate G-protein coupling to the bombesin receptor: direct evidence for biased agonism. *J Biol Chem* **276**:28083–28091.
- Maeda S, Sun D, Singhal A, Foggetta M, Schmid G, Standfuss J, Hennig M, Dawson RJ, Veprintsev DB, and Schertler GF (2014) Crystallization scale preparation of a stable GPCR signaling complex between constitutively active rhodopsin and G-protein. *PLoS One* **9**:e98714.
- Moeller HB, Rittig S, and Fenton RA (2013) Nephrogenic diabetes insipidus: essential insights into the molecular background and potential therapies for treatment. *Endocr Rev* **34**:278–301.
- Namkung Y, Le Gouill C, Lukashova V, Kobayashi H, Hogue M, Khoury E, Song M, Bouvier M, and Laporte SA (2016) Monitoring G protein-coupled receptor and  $\beta$ -arrestin trafficking in live cells using enhanced bystander BRET. *Nat Commun* **7**:12178.
- Namkung Y, LeGouill C, Kumar S, Cao Y, Teixeira LB, Lukasheva V, Giubilaro J, Simões SC, Longpré J-M, Devost D et al. (2018) Functional selectivity profiling of the angiotensin II type 1 receptor using pathway-wide BRET signaling sensors. *Sci Signal* **11**:eaat1631.
- Nuber S, Zabel U, Lorenz K, Nuber A, Milligan G, Tobin AB, Lohse MJ, and Hoffmann C (2016)  $\beta$ -Arrestin biosensors reveal a rapid, receptor-dependent activation/deactivation cycle. *Nature* **531**:661–664.
- Oakley RH, Laporte SA, Holt JA, Caron MG, and Barak LS (2000) Differential affinities of visual arrestin, beta arrestin1, and beta arrestin2 for G protein-coupled receptors delineate two major classes of receptors. *J Biol Chem* **275**:17201–17210.
- Okashah N, Wan Q, Ghosh S, Sandhu M, Inoue A, Vaidehi N, and Lambert NA (2019) Variable G protein determinants of GPCR coupling selectivity. *Proceedings of the National Academy of Sciences*.
- Okashah N, Wright SC, Kawakami K, Mathiasen S, Zhou J, Lu S, Javitch JA, Inoue A, Bouvier M, and Lambert NA (2020) Agonist-induced formation of unproductive receptor-G<sub>12</sub> complexes. *Proc Natl Acad Sci USA* **117**:21723–21730.
- Perroy J, Pontier S, Charest PG, Aubry M, and Bouvier M (2004) Real-time monitoring of ubiquitination in living cells by BRET. *Nat Methods* **1**:203–208.
- Rajagopal S (2013) Quantifying biased agonism: understanding the links between affinity and efficacy. *Nat Rev Drug Discov* **12**:483.
- Rajagopal S, Ahn S, Rominger DH, Gowen-MacDonald W, Lam CM, Dewire SM, Violin JD, and Lefkowitz RJ (2011) Quantifying ligand bias at seven-transmembrane receptors. *Mol Pharmacol* **80**:367–377.
- Rankovic Z, Brust TF, and Bohn LM (2016) Biased agonism: an emerging paradigm in GPCR drug discovery. *Bioorg Med Chem Lett* **26**:241–250.
- Rask-Andersen M, Masuram S, and Schiöth HB (2014) The druggable genome: evaluation of drug targets in clinical trials suggests major shifts in molecular class and indication. *Annu Rev Pharmacol Toxicol* **54**:9–26.
- Richard-Lalonde M, Nagi K, Audet N, Sleno R, Amraei M, Hogue M, Balboni G, Schiller PW, Bouvier M, Hébert TE et al. (2013) Conformational dynamics of Kir3.1/Kir3.2 channel activation via  $\delta$ -opioid receptors. *Mol Pharmacol* **83**:416–428.
- Rinschen MM, Schermer B, and Benzing T (2014) Vasopressin-2 receptor signaling and autosomal dominant polycystic kidney disease: from bench to bedside and back again. *J Am Soc Nephrol* **25**:1140–1147.
- Roberts DJ and Waelbroeck M (2004) G protein activation by G protein coupled receptors: ternary complex formation or catalyzed reaction? *Biochem Pharmacol* **68**:799–806.
- Qureshi S, Galiveeti S, Bichet DG, and Roth J (2014) Diabetes insipidus: celebrating a century of vasopressin therapy. *Endocrinology* **155**:4605–4621.
- Schönegge AM, Gallion J, Picard LP, Wilkins AD, Le Gouill C, Audet M, Stallaert W, Lohse MJ, Kimmel M, Lichtarge O et al. (2017) Evolutionary action and structural basis of the allosteric switch controlling  $\beta_2$ AR functional selectivity. *Nat Commun* **8**:2169.
- Smith JS, Lefkowitz RJ, and Rajagopal S (2018) Biased signalling: from simple switches to allosteric microprocessors. *Nat Rev Drug Discov* **17**:243–260.
- Smith JS, Pack TF, Inoue A, Lee C, Zheng K, Choi I, Eiger DS, Warman A, Xiong X, Ma Z et al. (2021) Noncanonical scaffolding of G<sub>ai</sub> and  $\beta$ -arrestin by G protein-coupled receptors. *Science* **371**:eaay1833.
- Sparapani S, Millet-Boureima C, Oliver J, Mu K, Hadavi P, Kalostian T, Ali N, Avelar CM, Bardies M, Barrow B et al. (2021) The biology of vasopressin. *Biomedicines* **9**:89.
- Stahl EL, Ehlert FJ, and Bohn LM (2019) Quantitating ligand bias using the competitive model of ligand activity, in *Methods in Molecular Biology* pp 235–247, Humana New York, NY.
- Steen A, Larsen O, Thiele S, and Rosenkilde MM (2014) Biased and g protein-independent signaling of chemokine receptors. *Front Immunol* **5**:277.
- Stefan E, Malleshiah MK, Breton B, Ear PH, Bachmann V, Beyermann M, Bouvier M, and Michnick SW (2011) PKA regulatory subunits mediate synergy among conserved G-protein-coupled receptor cascades. *Nat Commun* **2**:598.
- Szczepanska-Sadowska E, Wsol A, Cudnoch-Jedrzejewska A, and Żera T (2021) Complementary role of oxytocin and vasopressin in cardiovascular regulation. *Int J Mol Sci* **22**:11465.
- Tesmer JGG (2009) Chapter 4 structure and function of regulator of G protein signaling homology domains, in *Molecular Biology of RGS Proteins* pp 75–113.
- Traut TW (1994) Physiological concentrations of purines and pyrimidines. *Mol Cell Biochem* **140**:1–22.
- Uhlen M, Fagerberg L, Hallström BM, Lindskog C, Oksvold P, Mardinoglu A, Sivertsson Å, Kampf C, Sjöstedt E, Asplund A et al. (2015) Proteomics. tissue-based map of the human proteome. *Science* **347**:1260419–1260419.
- Vallar L, Muca C, Magni M, Albert P, Bunzow J, Meldolesi J, and Civelli O (1990) Differential coupling of dopaminergic D2 receptors expressed in different cell types. Stimulation of phosphatidylinositol 4,5-bisphosphate hydrolysis in Ltk-fibroblasts, hyperpolarization, and cytosolic-free Ca<sup>2+</sup> concentration decrease in GH4C1 cells. *J Biol Chem* **265**:10320–10326.
- van der Westhuizen ET, Breton B, Christopoulos A, and Bouvier M (2014) Quantification of ligand bias for clinically relevant  $\beta_2$ -adrenergic receptor ligands: implications for drug taxonomy. *Mol Pharmacol* **85**:492–509.
- Van Sande J, Raspé E, Perret J, Lejeune C, Maenhaut C, Vassart G, and Dumont JE (1990) Thyrotropin activates both the cyclic AMP and the PIP<sub>2</sub> cascades in CHO cells expressing the human cDNA of TSH receptor. *Mol Cell Endocrinol* **74**:R1–R6.
- Waelbroeck M, Boufrah L, and Swillens S (1997) Seven helix receptors are enzymes catalysing G protein activation. What is the agonist? *J Theor Biol* **187**:15–37.
- Wei H, Ahn S, Shenoy SK, Karnik SS, Hunyady L, Luttrell LM, and Lefkowitz RJ (2003) Independent beta-arrestin 2 and G protein-mediated pathways for angiotensin II activation of extracellular signal-regulated kinases 1 and 2. *Proc Natl Acad Sci USA* **100**:10782–10787.
- Xiao RP, Ji X, and Lakatta EG (1995) Functional coupling of the beta 2-adrenoceptor to a pertussis toxin-sensitive G protein in cardiac myocytes. *Mol Pharmacol* **47**:322–329.
- Zhu X, Gilbert S, Birnbaumer M, and Birnbaumer L (1994) Dual signaling potential is common among Gs-coupled receptors and dependent on receptor density. *Mol Pharmacol* **46**:460–469.
- Zimmerman B, Beautrait A, Aguilá B, Charles R, Escher E, Claing A, Bouvier M, and Laporte SA (2012) Differential  $\beta$ -arrestin-dependent conformational signaling and cellular responses revealed by angiotensin analogs. *Sci Signal* **5**:ra33.

---

**Address correspondence to:** Franziska M. Heydenreich, MRC Laboratory of Molecular Biology, Francis Crick Avenue, Cambridge CB2 0QH, United Kingdom. E-mail: franziskah@mrc-lmb.cam.ac.uk; Michel Bouvier, Department of Biochemistry and Molecular Medicine, Institute for Research in Immunology and Cancer, Université de Montréal, 2950, Chemin de Polytechnique Pavillon Marcelle-Coutu Montréal, Québec H3T 1J4 Canada. E-mail: michel.bouvier@umontreal.ca; or Dmitry B. Veprintsev, Division of Physiology, Pharmacology & Neuroscience, School of Life Sciences, University of Nottingham, Queen's Medical Centre, Nottingham NG7 2UH, United Kingdom. E-mail: dmitry.veprintsev@nottingham.ac.uk

---